

## RESEARCH ARTICLE

# Characterization and molecular targeting of CFIm25 (*NUDT21/CPSF5*) mRNA using miRNAs

Naazneen Khan<sup>1,2</sup>  | Mahesh Gupta<sup>1</sup>  | Chioniso Patience Masamha<sup>1</sup> 

<sup>1</sup>Department of Pharmaceutical Sciences, Butler University, Indianapolis, Indiana, USA

<sup>2</sup>Department of Neurology, Indiana University, Indianapolis, Indiana, USA

**Correspondence**

Chioniso Patience Masamha, Department of Pharmaceutical Sciences, Butler University, Indianapolis, IN 46208, USA.  
Email: [cmasamha@butler.edu](mailto:cmasamha@butler.edu)

**Funding information**

HHS | NIH | National Institute of General Medical Sciences (NIGMS), Grant/Award Number: R01 GM135361/GM/NIGMS

**Abstract**

Changes in protein levels of the mammalian cleavage factor, CFIm25, play a role in regulating pathological processes including neural dysfunction, fibrosis, and tumorigenesis. However, despite these effects, little is known about how CFIm25 (*NUDT21*) expression is regulated at the RNA level. A potential regulator of *NUDT21* mRNA are small non-coding microRNAs (miRNAs). In general, miRNAs bind to the 3'untranslated regions (3'UTRs) and can target the bound mRNA for degradation or inhibit translation thus affecting the levels of protein in cells. Interestingly, a mechanism known as alternative polyadenylation (APA) enables mRNAs to escape miRNA regulation by generating mRNAs with 3'UTRs of different sizes. As many miRNA target sites are located within the 3'UTR, shortening the 3'UTR allows mRNAs to evade miRNAs targeting this region. The differences in the lengths and the sequence composition of the 3'UTRs may also impact the mRNA's translatability and subcellular localization. APA has been reported to regulate over 70% of protein coding genes, thus increasing the transcript repertoire. Several proteins, including mammalian cleavage factor, CFIm25 (*NUDT21*), have been shown to regulate APA. In this study we wanted to determine whether CFIm25 (*NUDT21*), itself a regulator of APA, undergoes APA to evade miRNA regulation. We used the blood cancer mantle cell lymphoma (MCL) cells as a model and showed that in these cells, *NUDT21* is relatively stable with a long half-life. In addition, the *NUDT21* pre-mRNA undergoes alternative APA within the same terminal exon. The three different sized *NUDT21* mRNAs have different 3'UTR lengths and they each use a different canonical polyadenylation signal, AAUAAA, for 3'end cleavage and polyadenylation. Use of miRNA mimics and inhibitors showed that miR-23a, miR-222, and miR-323a play a significant role in regulating *NUDT21* expression. Hence, these results suggest that *NUDT21* mRNA is stable and the different 3'UTRs generated through APA of *NUDT21* play an important role in evading miRNA regulation and offers insights into how levels of CFIm25 (*NUDT21*) may be fine-tuned as needed under different physiological and pathological conditions.

This is an open access article under the terms of the [Creative Commons Attribution-NonCommercial-NoDerivs](https://creativecommons.org/licenses/by-nc-nd/4.0/) License, which permits use and distribution in any medium, provided the original work is properly cited, the use is non-commercial and no modifications or adaptations are made.

© 2025 The Author(s). *The FASEB Journal* published by Wiley Periodicals LLC on behalf of Federation of American Societies for Experimental Biology.

## 1 | INTRODUCTION

The RNA-binding protein and mammalian cleavage factor CFIm25 (*NUDT21*) is increasingly being recognized as an important regulator of normal biological processes including spermatogenesis, regulation of male fertility, embryonic development, and cell fate.<sup>1–5</sup> In humans, changes in CFIm25 protein levels are also associated with several pathological conditions including cancer, neuropsychiatric disorders and different types of fibrosis<sup>6–13</sup> (and reviewed<sup>14</sup>). Before these discoveries, CFIm25 was only believed to play a supportive role in 3'end formation. Formation of the 3'end occurs during pre-mRNA processing and involves 3'end cleavage and polyadenylation resulting in mature polyadenylated transcripts.<sup>15,16</sup> Among other roles, polyadenylation enables nuclear to cytoplasmic shuttling and translation of the polyadenylated mRNAs.<sup>17</sup> Although over 80 proteins have been found associated with the 3'end processing machinery, the core proteins consist of about 15 proteins that are subdivided into four major complexes in humans.<sup>15,16,18</sup> These consist of the mammalian cleavage factors I and II (CFIm and CFII), the cleavage stimulation factors (CstFs), and the cleavage and polyadenylation specificity factors (CPSFs).<sup>15,16</sup> Some members of these factors recognize and bind to specific sequence elements within the pre-mRNA. Wdr33 and CPSF30, bind to the polyadenylation signal which typically consists of the canonical hexanucleotide sequence AAUAAA.<sup>17,19</sup> Cstf64 (or CstF64 $\tau$ ) binds to a downstream G/U rich sequence.<sup>15,16</sup> CFIm25 binds to UGUA sequences and is recruited in the initial stages of 3'end formation. CFIm25 is believed to enhance 3'end cleavage and polyadenylation.<sup>20–22</sup> CFIm25 is a small 25 kilodalton protein that is encoded by the Nudix hydrolyase 21 gene (*NUDT21/CPSF5*). During 3'end formation, two CFIm25 subunits bind to a UGUA sequence on pre-mRNA and recruit either two CFIm59 or two CFIm68 subunits.<sup>23,24</sup> The CPSF73 endonuclease cleaves the pre-mRNA downstream of the polyadenylation signal and the 3'end is then polyadenylated.

Recent studies have shown that in addition to traditional 3'end formation, CFIm25 can regulate several other RNA processing events. These include regulating alternative splicing of pre-mRNAs, cyclization of circular RNAs, miRNA biogenesis and miRNA activity, as well as alternative polyadenylation (APA).<sup>6,25–30</sup> APA occurs when there are multiple polyadenylation signals within the same pre-mRNA that can be used for 3'end formation. APA allows the fine-tuning of over 70% of protein coding genes in the human genome.<sup>31</sup> Inhibition of APA in specific cancers may make them more vulnerable to treatments with DNA damage repair based therapies.<sup>32</sup> There are several types

of APA, some of which are linked to splicing. However, the most common type of APA occurs when the protein coding region is unaltered but there are changes in the length and sequence content of the 3'UTR due to usage of alternative polyadenylation signals within the same terminal exon.<sup>33</sup> These polyadenylation signals can be canonical (AAUAAA) or non-canonical.<sup>34</sup> Our study is focused on the latter type of APA which only involves changes in the size of the UTR, and we will refer to it as APA throughout the paper. The different 3'UTRs that are generated act as loading docks for several regulatory elements including RNA-binding proteins and miRNAs.<sup>35,36</sup> Hence, the size of the 3'UTR determines the sequence content which affects different aspects of mRNA metabolism including stability, translatability, as well as subcellular localization and thus function.<sup>37–40</sup> Reduction in the levels of CFIm25 (and other members of the CFIm complex) result in global shortening of the 3'UTRs of thousands of transcripts through APA.<sup>6,26,41</sup>

Despite the emerging roles of CFIm25 in normal biology and disease, the mechanisms that drive normal CFIm25 expression as well as CFIm25 dysregulation are not fully understood. Moreover, how CFIm25 (*NUDT21*) is regulated at the transcriptional, post-transcriptional level remains largely unknown. The goal of this study was to determine how this important regulator, CFIm25 (*NUDT21*) is itself regulated at the RNA level. To accomplish this, we used the hematological malignancy, mantle cell lymphoma (MCL) as a model to examine CFIm25 (*NUDT21*) transcript expression. MCL is a distinct subtype of non-Hodgkin's lymphoma (NHL) which follows an aggressive clinical pattern in up to 90% of the patients.<sup>42–44</sup> Before the advent of immunotherapy and other targeted therapies, MCL had a short remission period, was considered clinically incurable upon relapse and thus had the worst overall prognosis of all B-cell lymphomas.<sup>43,45–49</sup> Despite the use of targeted therapies, patients with drug-resistant disease or who have disease recurrence still have a poor clinical outcome.<sup>50</sup> Further understanding of MCL biology at the molecular level allowing for patient stratification is crucial for all MCL patients but especially those with relapsed or drug-resistant disease.<sup>50,51</sup> A subset of MCL patients with highly proliferative disease were observed to express the G1-S phase cell cycle rate-limiting oncogene, cyclin D1 (*CCND1*) transcripts with truncated 3'UTRs which reduced their survival by 2 years.<sup>52</sup> This shortening of the *CCND1* 3'UTR transcript was through APA due to mutations in the polyadenylation signal, deletions of a major section of the 3'UTR as well as chromosomal translocations resulting in a fusion transcript that only involves the *CCND1* 3'UTR. MCL cell lines have been identified that contain these diverse *CCND1* 3'UTRs making these

ideal model cell lines to study transcript diversity.<sup>52,53</sup> Furthermore, the aberrant chronic presence of cyclin D1 in MCL makes it the B-cell lymphoma with the highest level of genetic instability of all the B-cell lymphomas.<sup>54–56</sup> Hence, we posited that just like for *CCND1*, if there is any naturally occurring 3'UTR based transcript variation in our target, CFIm25 (*NUDT21*), this would be found in MCL cells due to their inherent nature that allows for the potential generation of alternate transcripts through diverse means. We used a combination of different techniques to determine the stability of *NUDT21* mRNAs, identify different *NUDT21* transcripts expressed in MCL cells, measure their expression levels based on differences in the 3'UTR as well as the impact of miRNA mimics and inhibitors on the 3'UTRs. Our experiments provide strong support that there is a drive for MCL cells to express *NUDT21* transcripts which are relatively stable and whose expression can be fine-tuned using miRNAs. As such, modulating the expression of CFIm25 (*NUDT21*) will have an impact on the biological and pathological processes it is now known to regulate.

## 2 | MATERIALS AND METHODS

### 2.1 | Cell culture

We purchased the MCL cell lines Jeko-1 (ATCC CRL-3006), Mino (ATCC CRL-3000), Z-138 (ATCC CRL-3001), and Rec-1 (ATCC CRL-3004) from the American Tissue Culture Collection (ATCC) (Manassas, VA, USA). We also used the Granta-519 MCL cell line (Cat# ACC 342, DSMZ-German Collection of Microorganisms and Cell Cultures, GmbH, Germany). In addition to the MCL cell lines we also used the HeLa cell line (Cat# ATCC CCL-2, ATCC Manassas, VA, USA) for some of our assays. Cells were grown in DMEM with GlutaMAX (Cat# 10569044 ThermoFisher Scientific, Carlsbad, CA, USA) supplemented with 10% fetal bovine serum (Cat# 16140071, ThermoFisher Scientific, Carlsbad, CA, USA) and 1% Penicillin—Streptomycin (Cat# 15070063, ThermoFisher Scientific, Carlsbad, CA, USA). Cells were cultured at 37°C in a 5% CO<sub>2</sub> incubator.

### 2.2 | RNA extraction and PCR primers

After cell culture and appropriate treatment, total RNA was harvested using TRIzol<sup>®</sup> reagent (Cat# TRIzol<sup>®</sup> Reagent, Invitrogen<sup>™</sup>, ThermoFisher Scientific, Carlsbad, CA, USA) using the manufacturer's protocol. The RNA was then reverse transcribed using RevertAid first strand cDNA synthesis kit (Cat#

K1622, ThermoFisher Scientific, Carlsbad, CA, USA). For qRT-PCR the random hexamer primer was used for reverse transcription while the oligo(dT)18 primer (both from the kit) was used for 3'Rapid Amplification of cDNA ends (3'RACE). Primers to measure total levels of *NUDT21* within the open reading frame were forward GAGAAGGACAGCTCTGTTGCAGCCA and reverse TGCAGCTACCAGCTTGTA. The primers used to measure *NUDT21* long 3'UTRs located downstream of the PAS2 near the distal PAS3 were forward CAGTACTTGTTTCAGTCACTTGAG and reverse GATACAAAATACACCTGAACTGGC. The design of primers to measure total mRNAs and mRNAs with long 3'UTRs was previously described.<sup>6</sup> Primers for *GAPDH* qRT-PCR were forward TGACTTCAACAGCGACACCCA and reverse CACCCTGTTGCTGTAGCCAAA.

### 2.3 | 3'rapid amplification of cDNA ends

We performed 3'RACE with the reverse primers oligo(dT)25 T7 used for the first nested PCR and the T7 primer for the second round of PCR as we previously described.<sup>53,57</sup> The two sets of forward nested primers used to detect the first polyadenylation signal (PAS1) 3'UTR of *NUDT21* were primer 1, TCACTCAGTTCGGCAACAAG and primer 2, GAGAAGGACAGCTCTGTT. Forward nested primers used for PAS2 were primer 1, GAAGAACTAGATAGTGGTGTAAC and primer 2, TACCATTCTTGGGCACATACTC. The forward primers used for PAS3 were primer 1, GGACAAAGTGTGACCAAATTAGCC and primer 2, ATTCAACAGGCCAGCAAGC.

### 2.4 | Cloning and Sanger sequencing

After 3'RACE, the PCR products were run on a gel and after gel extraction, we used the Zero Blunt TOPO PCR cloning kit (Cat# K280020, ThermoFisher Scientific Carlsbad, CA, USA) to perform topoisomerase-based cloning as per manufacturer's protocol. Positive clones were screened using restriction enzyme digestion and sent for Sanger Sequencing at LoneStar Labs (Houston, TX, USA).

### 2.5 | Inhibition of translation with actinomycin D

To determine mRNA stability, we treated our suspension cells with 10ug/ml of actinomycin (Cat# DSBR00013, Sigma-Aldrich, St. Louis, MO, USA) and collected samples

over time as previously reported with slight modifications that included plating  $1 \times 10^6$  cells in 6-well plates for treatment.<sup>58</sup> RNA extraction and cDNA synthesis were conducted as described in Section 2.2.

## 2.6 | Plasmid and miRNA mimic/inhibitor transfection and luciferase assays

The full-length 3'UTR of *NUDT21* was cloned into the psiCHECK2 dual luciferase vector (Cat# C8021, Promega, Madison, WI, USA) downstream of the synthetic Renilla luciferase gene (Rluc) between XhoI and NotI.<sup>53,59</sup> HeLa cells were plated into 12-well plates (190 000 cells/well) and after 4 h, cells were transfected with 200 ng per well of plasmid using Lipofectamine 2000 (Cat# 11668019, Invitrogen part of ThermoFisher Scientific, Carlsbad, CA, USA). After 24 h, the media was changed and cells were transfected with 20 nM of the miRNA mimic negative control (Cat# 4464058), and either the miRNA mimic or miRNA inhibitor for each of the following hsa-miR-23a-3p (mimic (MC10644) and inhibitor (MH10644)), hsa-miR-27b-3p (mimic (MC10750) and inhibitor (AM10750)), hsa-miR-181b-5p (mimic (MC12442) and inhibitor (AM12442)), hsa-miR-222-3p (mimic (MC11376) and inhibitor (MH11376)), hsa-miR-323a-3p (mimic (MC12418) and inhibitor (MH12418)).<sup>53,59</sup> All the miRNA mimics and inhibitors were purchased from Life Technologies (a part of ThermoFisher Scientific, Carlsbad, CA, USA). The next day the media was changed, and the cells were transfected for the second time with the miRNA mimics or inhibitors. All the miRNA inhibitor or mimic transfections were done in quadruplicate. Twenty-four hours after this second transfection, cells were harvested and assayed using the Dual-Luciferase® Reporter Assay System (Cat# E1910, Promega, Madison, WI, USA) as per manufacturer's instructions.

## 2.7 | Measuring effects of miRNA on endogenous *NUDT21*

For qRT-PCR of endogenous *NUDT21*, HeLa cells were plated in 6-well plates (300 000 cells/well). After four hours, cells were transfected with miR-222-3p mimic or inhibitor (as previously described in Section 2.6) using Lipofectamine 2000 (Cat# 11668019, Invitrogen part of ThermoFisher Scientific, Carlsbad, CA, USA). Twenty-four hours later, the media was changed, and transfection was done a second time. Total RNA was extracted from cells 48 h after the second transfection, and qRT-PCR was carried out for *NUDT21* and *GAPDH*.

## 2.8 | Transduction and MTT assays

Transduction of Jeko-1 and Granta-519 cells was done using hexadimethrine bromide (Cat# H9268, MilliporeSigma, St. Louis, MO, USA) per manufacturers' protocol. We used 3'UTR targeted *NUDT21* shRNA clone ID TRCN0000000145 (Cat# SHCLNV, NM\_007006, Sigma-Aldrich, MilliporeSigma, St. Louis, MO, USA), and control MISSION® pLKO.1-puro-UbC-TurboGFP™ Positive Control Plasmid (Cat# SHC014, MilliporeSigma, St. Louis, MO, USA). Eight days after starting puromycin (Cat# P9620, MilliporeSigma, St. Louis, MO, USA) selection, cells were plated in 96-well plates (20 000 cells/well). After 72 h, we performed the MTT assay (Cat# ATCC® 30-1010K, ATCC Manassas, VA, USA) as previously described.<sup>59</sup>

## 2.9 | Western Blot

After shRNA (as previously described in Section 2.8), cell pellets were collected and lysed with M-PER™ Mammalian Protein Extraction Reagent (Cat# 78503 ThermoFisher Scientific, Carlsbad, CA, USA) and protein was resolved on an 8% SDS-PAGE gel and transferred to a PVDF membrane. After blocking for 1 h at room temperature with 5% non-fat milk resuspended in phosphate buffered saline (with 0.001% Tween 20), the membrane was probed with primary antibodies against the CFIm25 protein using rabbit anti *NUDT21* (1:1000 overnight at 4°C) polyclonal antibody (Cat# 10322-1-AP, Proteintech Rosemont, IL, USA) and GAPDH (1:5000 for 1 h) using Anti-GAPDH antibody [EPR6256] (Cat# ab128915, Abcam Waltham, MA, USA). For detection, the membrane was probed with Goat anti-Rabbit IgG (H+L), Superclonal™ Recombinant Secondary Antibody, Alexa Fluor 680 (at 1:5000 for 1 h-Cat# A27042, Invitrogen a part of ThermoFisher Scientific, Carlsbad, CA, USA).

## 2.10 | Statistics

GraphPad Prism software was used to analyze the results (Student's independent *t*-test where  $n \geq 3$ ,  $p < .05$ ).

# 3 | RESULTS

## 3.1 | Determination of *NUDT21* mRNA stability in MCL

Despite the ability of the CFIm25 protein to regulate the 3'UTR through alternative polyadenylation (APA) for

thousands of genes and affect mRNA stability, not much is known about the stability of its *NUDT21* mRNA. To determine the stability of the *NUDT21* mRNA we used the MCL cell lines, Jeko-1 and Z-138 cell lines whose *CCND1* mRNAs arising from very different mechanisms are well documented, as well as the Mino cell line whose *CCND1* transcripts are unknown.<sup>52,53</sup> We treated the cells using actinomycin D to inhibit transcription and performed qRT-PCR to determine the total levels of *NUDT21* transcripts at different timepoints.<sup>60</sup> The levels of *NUDT21* mRNA remained high with 70% of the transcript still present after 4 h in both the Mino and Z-138 MCL cell lines (Figure 1). After 8 h, Mino still had 60% of the *NUDT21* transcript while 54% remained in Z-138 cells. In Jeko-1 cells 54% of the *NUDT21* transcript was present 4 h after treatment with actinomycin D and after 8 h, 21% of the transcript remained.

### 3.2 | Identification of different *NUDT21* mRNA 3'UTRs and polyadenylation signals used

A previous study in the HeLa model cell line identified three different *NUDT21* mRNAs containing the same open reading frame, but different sized 3'UTRs.<sup>61</sup> This was the first indication that *NUDT21* pre-mRNAs can undergo APA. To determine the diversity of *NUDT21* transcripts, we expanded the number of cell lines we screened to five MCL cell lines. The cell lines have different sensitivities to anti-cancer drugs and different molecular profiles.<sup>62-64</sup> In terms of *CCND1*, the Jeko-1 and Z-138 cell lines contain *CCND1* transcripts with short and long 3'UTRs resulting from APA driven by mutations that generate a canonical polyadenylation signal proximal to

the open reading frame.<sup>52,53</sup> The Granta-519 cell line expresses a 3'UTR *CCND1* truncated fusion transcript with the fusion gene partner sequences from *CDC42BPA/MRCK* fused to sequences within the *CCND1* 3'UTR. A canonical polyadenylation signal, AAUAAA derived from the fused *CDC42BPA/MRCK* sequence is used for 3'end formation.<sup>53</sup> Although Rec-1 and Mino MCL cell lines express cyclin D1 protein, the nature of their *CCND1* transcripts is not well defined.<sup>65</sup> We performed 3'end rapid amplification of cDNA ends (3'RACE) for *NUDT21* and ran the Jeko-1, Granta-519, Rec-1, Mino and Z-138 PCR products on an agarose gel. Three different sized 3'UTRs were present in all the five MCL cell lines similar to those found in HeLa cells. These three transcripts were due to usage of the polyadenylation signal most proximal to the open reading frame (PAS1), an intermediate polyadenylation signal (PAS2) and a distal polyadenylation signal (PAS3) all within the same terminal exon (Figure 2A). When we performed Sanger sequencing, we found that all the three polyadenylation signals are identical consisting of the canonical hexanucleotide AAUAAA (Figure 2B). We also compared the full-length reference *NUDT21* sequence from Ensembl genome browser (*NUDT21*-201 ENST00000300291.10) to the Sanger sequences we obtained for all five MCL cell lines for 3'RACE PCR products from PAS1, PAS2, and PAS3 using the multiple sequence alignment software (MUSCLE). We found that the AAUAAA canonical hexamer was conserved for each PAS in all the cell lines (Figure S1-C).

### 3.3 | Quantifying differences in levels of mRNAs containing short and long 3'UTRs

To compare the usage of the different polyadenylation signals in *NUDT21*, we developed primers that target the open reading frame (ORF) and give total mRNA levels, as well as primers that only target the distal full-length 3'UTR allowing measurement of mRNAs with full-length 3'UTRs only as previously described.<sup>6</sup> A schematic showing the relative location of the primers for qRT-PCR is provided (Figure 3A). Our qRT-PCR results consistently show that in all the cell lines, there are much lower levels of mRNAs containing full-length 3'UTRs and that the most distal polyadenylation signal (PAS3) is used less than the other polyadenylation signals (PAS2 and PAS1) (Figure 3B). Our primers are unable to distinguish between usage of PAS1 and PAS2 which are more proximal to the open reading frame. Hence, in MCL cells *NUDT21* undergoes APA to preferentially generate *NUDT21* mRNAs with shorter 3'UTRs.

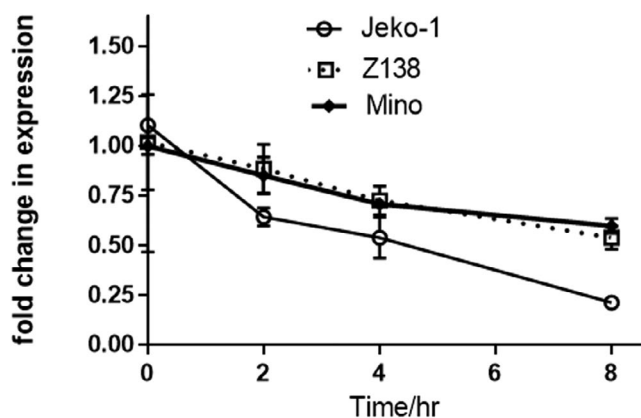
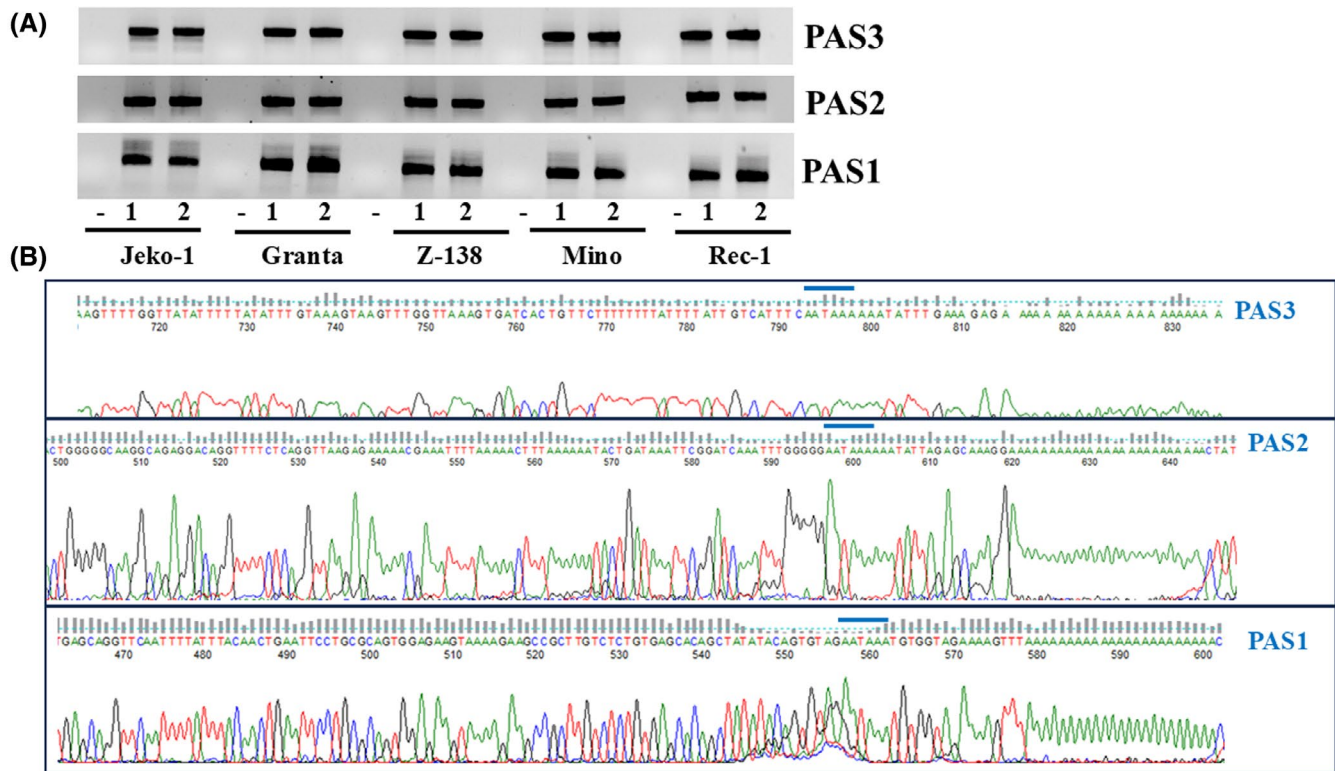


FIGURE 1 *NUDT21* mRNA levels over time. qRT-PCR of *NUDT21* levels after actinomycin D treatment. Fold change in expression was normalized to levels of GAPDH. Data shown are the mean  $\pm$  SD of three biological replicates.



**FIGURE 2** Characterization of *NUDT21* mRNAs. (A) Ethidium bromide-stained agarose gel showing the 3' rapid amplification of cDNA end (3' RACE) products of RNA extracts from five mantle cell lymphoma cell lines. The products obtained from usage of the first polyadenylation signal (PAS1), second polyadenylation signal (PAS2) and third polyadenylation signal (PAS) in each cell line are shown in duplicate together with the negative control (-). (B) Sanger sequencing chromatograms after 3' RACE showing the location of the polyadenylation signals (shown by blue line for PAS1, PAS2, PAS3).

### 3.4 | Determining the impact of miRNAs on the 3'UTR of *NUDT21*

Alternative polyadenylation plays many roles including evading miRNA regulation and increasing the stability of specific transcripts.<sup>66</sup> In order to determine the role of miRNAs in regulating the *NUDT21* 3'UTR, we used miRwalk (Figure S2)<sup>67,68</sup> and Starbase v2.0/the Encyclopedia of RNA interactomes (ENCORI) (Figure S3)<sup>69,70</sup> to identify potential miRNA-binding sites on the *NUDT21* transcript. The relative locations of select miRNA target sites within the *NUDT21* 3'UTR and polyadenylation signals (PAS) are also shown (Figure 3A).

To determine the impact of select miRNAs on the *NUDT21* 3'UTR, we then cloned the full-length 3'UTR of *NUDT21* into a pscheck-2 dual luciferase reporter plasmid. We did transient transfection of the reporter plasmid into HeLa cells which also express the same endogenous *NUDT21* transcripts as MCL cells, as MCL cell lines, similar to other lymphoma and leukemia cell lines, are as notoriously difficult to transfect for gene expression and have a low transfection efficiency.<sup>71,72</sup> Use of the

more easily transfected HeLa cells eliminates variability in transfection efficiency. After additional transfection of a miRNA mimic or inhibitor, the Renilla luciferase activity was measured and normalized it to Firefly luciferase activity. Treatment with the miR-23a mimic did not result in a significant change in luciferase activity, however treatment with the miR-23a inhibitor resulted in a significant increase in luciferase activity relative to the control (Figure 4A). There were no significant changes in luciferase activity after treatment with either the miR-27b mimic or inhibitor (Figure 4B). Although there was a slight decrease in luciferase activity after treatment with the miR-181b mimic, this was not accompanied by an increase in luciferase activity after treatment with the inhibitor (Figure 4C). Treatment with either the miR-222 (Figure 4D) or miR-323a mimics (Figure 4E) resulted in a significant decrease in luciferase activity. Treatment with the inhibitor for each miRNA resulted in a significant increase in luciferase activity. To determine the effects of miR-222 mimic and inhibitor on endogenous *NUDT21* transcripts, we transfected them into HeLa cells and performed qRT-PCR. We found that the miR-222 mimic

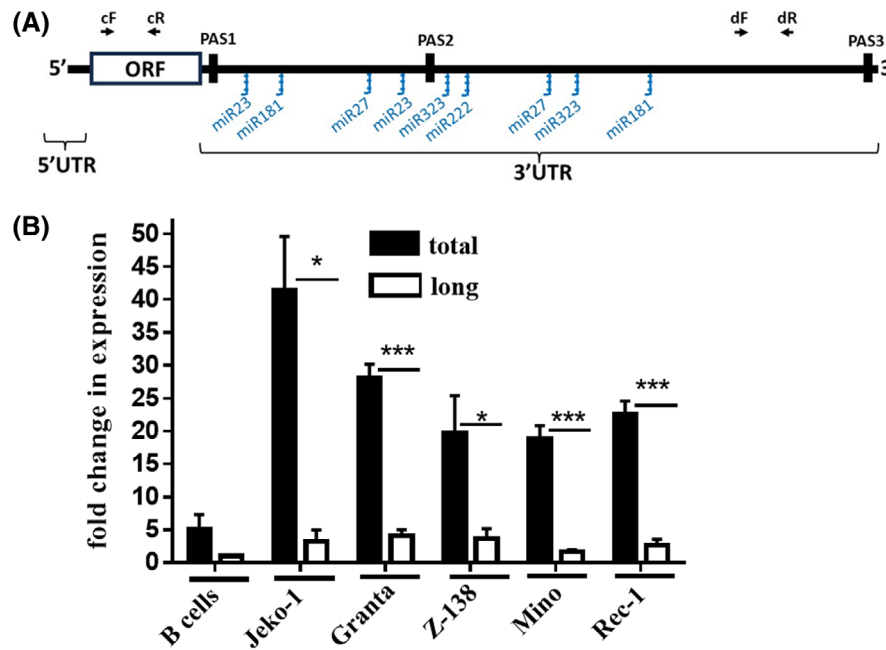


**FIGURE 3** Alternative polyadenylation resulting in differences in 3'UTR length in mantle cell lymphoma. (A) Schematic representation showing the relative location of the polyadenylation signals (PASs), and the primers used for qRT-PCR. The relative location of the binding sites of select miRNAs within the 3'UTR is also shown. The NUDT21 sequence this is based on was obtained from Ensembl (Transcript ID in Ensembl ENST00000300291.10 NUDT21-201, RefSeq Match NM\_007006.3). (B) qRT-PCR results showing fold changes in expression of total NUDT21 mRNAs when compared to the long mRNAs in B cells. Results were normalized to levels of GAPDH. Data shown is the mean  $\pm$  SD of three biological replicates. Statistical representation shown is \* $p < .05$ ; \*\*\* $p < .0001$  from Student *t*-tests.

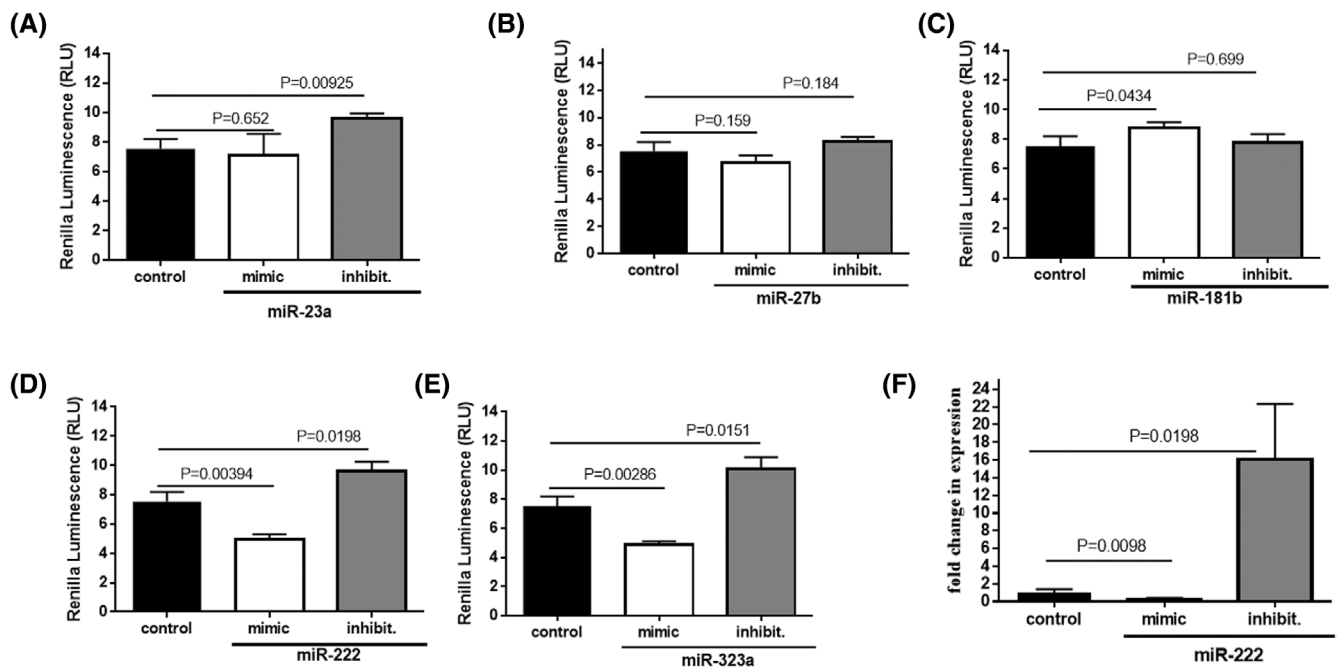


**FIGURE 4** Effect of miRNA mimics on the NUDT21 3'UTR. Normalized relative luminescence units (RLU) of HeLa cell transfected with the psiCHECK2 dual luciferase plasmid containing the full-length NUDT21 3'UTR after treatment with negative control miRNA mimic (control), a specific miRNA mimic or miRNA inhibitor (inhibit.). Shown is data for (A) hsa-miR-23a, (B) hsa-miR-27b-3p, (C) hsa-miR-181b, (D) hsa-miR-222-3p, and (E) hsa-miR-323a-3p. Representative data are shown of experiments done on the same day with three biological triplicates all normalized to the same control. (F) qRT-PCR results of endogenous NUDT21 levels after treatment of HeLa cells with hsa-miR-222-3p mimic and inhibitor.

resulted in a decrease in endogenous *NUDT21* levels while the miR-222 inhibitor resulted in an increase in endogenous *NUDT21* levels (Figure 4F).

### 3.5 | Determining the impact of the loss of full-length 3'UTR *NUDT21* mRNAs using 3'UTR targeted shRNA

In order to determine the potential role of the *NUDT21* mRNAs with the longest 3'UTRs in MCL, we initially used siRNA to target the *NUDT21* 3'UTR in MCL cells using a nucleofection protocol we had successfully used before in the MCL cell lines Jeko-1 and Granta-519, to target *CCND1* transcripts and cyclin D1 protein expression,<sup>53</sup> but did not detect any decrease in CFIm25 protein (results not shown). As MCL cells are known to be difficult to transfect,<sup>72</sup> we used specific shRNA targeting the 3'UTR to knock out *NUDT21* mRNA in Jeko-1 and Granta-519. We then performed MTT proliferation assays. We found that *NUDT21* depletion resulted in increased cell proliferation in both Jeko-1 ( $p = 7.52 \times 10^{-17}$ ) and Granta-519 ( $p = 6.8 \times 10^{-6}$ ) when compared to control (Figure 5A,B). Interestingly despite increased cell proliferation, there was only a 17% reduction in protein levels in Jeko-1 (Figure 5C) and a 39% decrease in protein levels in

Granta-519 (Figure 5D) after using shRNA targeting the *NUDT21* 3'UTR.

## 4 | DISCUSSION

Despite the impact of CFIm25 in cancer and other biological and physiological processes (as recently reviewed<sup>14</sup>), how the expression of CFIm25 is regulated still remains an active area of research. In a recent study, the *NUDT21* protein, CFIm25, was posited to play a role in independently regulating transcription.<sup>5</sup> A previous study of mRNA half-life measurements showed that in general, the half-lives of transcription and other related factors were less than one hour.<sup>73</sup> To determine the stability of *NUDT21* transcripts we treated cells with actinomycin D and performed qRT-PCR. Our results show that in contrast to transcription factors, *NUDT21* mRNA is relatively stable. This agrees with observations made so far that the effects of CFIm25 in cell biology in vivo do not seem to be related to drastic changes in its expression but may be associated with tightly regulated slight changes in its levels. The stability of the *NUDT21* mRNA suggests that in the cell there are mechanisms normally in place to keep levels of the *NUDT21* mRNA and protein stable underscoring its essential roles within the cell.

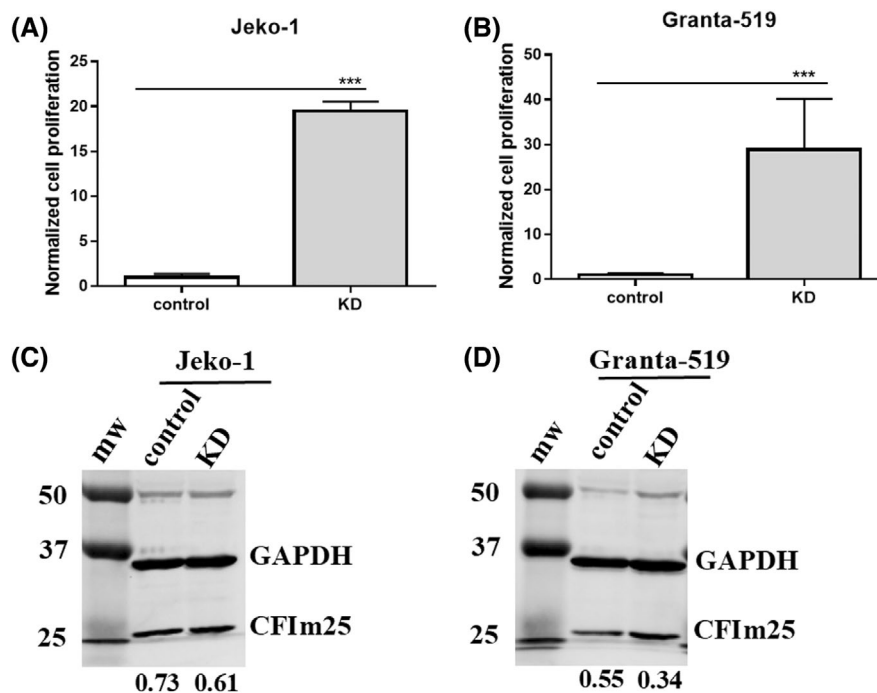


**FIGURE 5** Effects of CFIm25 (*NUDT21*) depletion in mantle cell lymphoma. Graphs depicting cell proliferation as determined by MTT assays after depletion (KD) of *NUDT21* using shRNA in (A) Jeko-1 and (B) Granta-519 cells. Results were normalized to control. Western Blot results after probing control and *NUDT21* shRNA transduced Jeko (C) and Granta-519 (D) cell lysates with antibodies to detect CFIm25 protein and GAPDH. Shown is the control shRNA and *NUDT21* shRNA (KD). Densitometric quantification of bands was performed using Image Lab Software (Bio-Rad) and the levels of CFIm25 normalized to that of the GAPDH is shown for each lane. \*\*\* $p < .0001$  from Student *t*-tests.

CFIm25 (*NUDT21*) is a member of the 3' end processing machinery and until recently was known in its traditional role in 3' end cleavage and polyadenylation. In addition to 3' end formation, CFIm25 and some members of the 3' end processing machinery have been shown to be involved in regulating transcript diversity through an emerging form of gene regulation known as alternative polyadenylation (APA). APA allows for the generation of transcripts containing the same open reading frame but different sized 3'UTRs thus greatly contributing to transcript diversity. The length of the 3'UTR and the sequences it contains may affect the subcellular localization and subcellular translation of the different sized transcripts, as well affect the transcripts translatability and stability. How APA is regulated is still being elucidated. Downregulation of several other 3' end processing factors has been shown to regulate APA. Reduction in levels of the CFIm member Pcf11 resulted in widespread lengthening of the 3'UTR.<sup>74</sup> Loss of Fip1, CstF64 as well as its paralog CstF64 $\tau$  also resulted in generation of transcripts with long 3'UTRs.<sup>6,75,76</sup> Reduction in levels of the CFIm complex including CFIm68, CFIm59, and CFIm25 resulted in global shortening of 3'UTRs.<sup>26,41</sup> Compared to the other 3' end processing factors, in general, genome-wide shortening of 3'UTRs after CFIm25 (*NUDT21*) knockdown has been shown to have the most impact on cellular physiology and has been associated with increased cell proliferation, increased tumorigenesis and larger tumor size in mouse xenograft models of solid cancer.<sup>6-8,77</sup> As the CFIm25 protein regulates APA, we wanted to determine whether *NUDT21* transcripts also undergo APA. Our work showed that CFIm25 is post-transcriptionally regulated through APA of the *NUDT21* pre-mRNA giving rise to three different transcripts in all five MCL cell lines. The occurrence of different sized *NUDT21* transcripts, which only differ in their 3'UTR lengths, in MCL is consistent with the findings in HeLa cells.<sup>61</sup> Interestingly, all three transcripts are due to usage of the same canonical polyadenylation signal consisting of the hexanucleotide, AAUAAA, which is optimal for 3' end cleavage and polyadenylation.<sup>34</sup> In this case, the sequence of the polyadenylation signal is not expected to be the main driver of the polyadenylation signal used for APA. Other cis and/or trans signals surrounding the polyadenylation signal may play a more important role in regulating APA of *NUDT21*. This includes the numerous UGUA sequences found throughout the *NUDT21* transcript or downstream U/GU-rich elements.<sup>78,79</sup> Binding of transcription factors to enhancers may also play a role in cleavage and polyadenylation site choice when the polyadenylation signals are identical.<sup>80</sup> The redundancy in the sequence of the three canonical polyadenylation signals used in generating the *NUDT21* transcripts suggests that based on the polyadenylation signals alone, there is an

innate drive to generate polyadenylated *NUDT21* transcripts regardless of the size of the 3'UTR. Our results showed that levels of *NUDT21* mRNAs with the longest 3'UTR were much lower than those with the shorter 3'UTRs. As the *NUDT21* pre-mRNA has numerous UGUA which are potential CFIm25-binding sites, it cannot be ruled out that the protein may play a role in its own APA. Thus, *NUDT21* undergoes APA, and this may function as a mechanism to regulate its expression.

Reduction of the 3'UTR length through APA eliminates destabilizing sequences as well as miRNA target sites localized within the longer 3'UTR. Apart from enabling the transcripts to evade regulation by target miRNAs hence increasing their stability, the miRNAs are now available to target other transcripts for degradation.<sup>81</sup> To experimentally identify miRNAs that target the *NUDT21* 3'UTR, we used several miRNA mimics and inhibitors in cells transfected with the *NUDT21* 3'UTR dual luciferase plasmid. The ability of the synthetic miR-23a inhibitor to increase luciferase activity suggests that the inhibitor was able to bind to endogenous miR-23a and function as a molecular sponge. The inability of the miR23a-mimic to reduce luciferase activity suggests that in HeLa cells, the dual luciferase reporter containing the *NUDT21* 3'UTR already have maximal endogenous miR-23a bound to it. This confirms previous findings that miR-23 regulates *NUDT21*.<sup>82</sup> Supplementing endogenous miRNAs, miR-222 and miR-323a with their respective mimics significantly decreased luciferase activity showing that these two miRNAs play a key role in regulating the *NUDT21* mRNA and this is further supported by the effects of their respective inhibitors which increased luciferase activity. Furthermore, use of the miR-222 mimic and inhibitor also resulted in similar changes in the endogenous *NUDT21* levels as shown by qRT-PCR. Thus, our experiments validated that miR-23a, miR-323a and miR-222 are important regulators of *NUDT21*. This is in addition to several other miRNAs that have been previously shown to target *NUDT21*.<sup>82</sup> Though this offers mechanistic insights into miRNA regulation, it is unknown if these miRNAs would have the same impact under normal physiological conditions or in MCL in vivo. More recently, another study showed that miR-181a and miR-181b regulate *Nudt21* in a mouse model bleomycin-induced dermal fibrosis further underscoring the interest in and the importance of understanding *NUDT21* regulation.<sup>9</sup> The different miRNAs that target *NUDT21* may allow for cell specific and/or context specific regulation and fine-tuning of *NUDT21* mRNAs and hence CFIm25 protein expression.

Individuals with *NUDT21* duplications or deletions had intellectual disabilities.<sup>13</sup> Reduced levels of CFIm25 protein in *Nudt21*<sup>+/-</sup> mice resulted in learning deficits.<sup>12</sup> This suggests that there is a level of CFIm25 protein

expression required for normal brain development and other physiological processes. To determine the effects of losing *NUDT21* transcripts with the full-length 3'UTR on cell survival we used RNAi targeting the 3'UTR. When we used siRNA to target the *NUDT21* 3'UTR in MCL cells using a nucleofection protocol we had used before<sup>53</sup> we did not detect any changes in *CFIm25* protein levels. Due to well documented challenges associated with transfecting MCL cells<sup>72</sup> we used shRNA targeting the 3'UTR region to knock out *NUDT21* mRNA. We found that depletion of *CFIm25* (*NUDT21*) in the MCL cell lines, Jeko-1 and Granta-519, resulted in increased cell proliferation. This was despite only a slight decrease in the *CFIm25* protein levels. A similar increase in cell proliferation, after *CFIm25* knockdown, has been reported for other tumors including cervical cancer cell lines<sup>6,8</sup> and hepatocellular carcinoma cell lines<sup>29,83</sup> after targeting the open reading frame using RNAi. Hence, like these solid cancers, *CFIm25* levels may play an important tumor suppressive role. The slight decrease in *CFIm25* after shRNA targeting the 3'UTR may correspond to the low levels of full-length 3'UTR *NUDT21* we initially detected using qRT-PCR in the MCL cell lines. However, dosage compensation at the protein level through some unknown mechanism cannot be ruled out. Interestingly, a previous study in *Nudt21*<sup>+/-</sup> mice, found that although the *Nudt21* mRNA levels were decreased by 50%, there was partial compensation at the protein level with only a 30% decrease in *CFIm25* the protein levels.<sup>12</sup> This potential aspect of specific dosage compensation suggests that levels of *CFIm25* are tightly regulated in a tissue- or state-specific manner. Our results suggest that even a slight reduction in levels of *NUDT21* full-length transcripts is sufficient to alter the cell phenotype. Hence, fine-tuning of *CFIm25* protein levels in MCL may affect tumorigenesis and other biological states. Further studies to uncover how slight changes in *NUDT21* mRNAs affect the *CFIm25* protein levels and how this is normally triggered in cell biology still need to be done.

The increasing repertoire of the different molecular roles of *CFIm25* in normal cellular processes and its involvement in human diseases behooves further studies in how it is regulated in vivo. Furthermore, *CFIm25*'s emerging role in tumorigenesis, either as tumor suppressor, or an oncogene based on the cancer, makes it a viable therapeutic target.<sup>6,84-86</sup> There is interest in developing therapeutics that regulate 3'end processing factors, including *CFIm25*, and the discovery of a compound JTE-607, which inhibits the activity of the 3'end factor CPSF73, suggests that targeting and regulating 3'end factors, including *CFIm25*, may have therapeutic applications in the disease state.<sup>32</sup> In conclusion, our experimental results suggest that APA of *NUDT21* resulting in the presence of different sized

3'UTRs allows for the fine-tuning of *NUDT21* mRNA levels by evading miRNAs as needed to maintain *CFIm25* protein levels in cells that are needed to maintain normal cellular physiology.

## AUTHOR CONTRIBUTIONS

Chioniso Patience Masamha conceived the study and designed the experiments. Naazneen Khan, Mahesh Gupta, and Chioniso Patience Masamha performed the experiments and did the data analysis. Chioniso Patience Masamha wrote the draft manuscript. Chioniso Patience Masamha and Naazneen Khan edited the manuscript. We would also like to acknowledge members of the Masamha lab for their careful reading of this manuscript.

## ACKNOWLEDGMENTS

The work presented in this manuscript was funded by the National Institutes of Health (NIH) Grant # R01 GM135361/GM/NIGMS awarded to CPM.

## DISCLOSURES

The authors have no conflicts of interest to disclose.


## DATA AVAILABILITY STATEMENT

All the data that were generated and analyzed in this study are included in the published article (and provided [supplementary files](#)) and are openly available in NCBI GenBank under the following accession numbers: PQ072305, PQ072306, PQ072307, PQ072307, PQ072308, PQ072309, PQ072310, PQ072311, PQ072312, PQ072313, PQ072314, PQ072315, PQ072316, PQ072317, PQ072318, and PQ072319.

## ORCID

Naazneen Khan  <https://orcid.org/0000-0002-4386-1703>

Mahesh Gupta  <https://orcid.org/0000-0001-9440-5364>

Chioniso Patience Masamha  <https://orcid.org/0000-0002-2427-786X>

## REFERENCES

- Sartini BL, Wang H, Wang W, Millette CF, Kilpatrick DL. Pre-messenger RNA cleavage factor I (CFIm): potential role in alternative polyadenylation during spermatogenesis. *Biol Reprod.* 2008;78(3):472-482.
- Brumbaugh J, di Stefano B, Wang X, et al. Nudt21 controls cell fate by connecting alternative polyadenylation to chromatin signaling. *Cell.* 2018;172(1):106-120.e21.
- Li H, Frappart L, Moll J, et al. Impaired planar germ cell division in the testis, caused by dissociation of RHAMM from the spindle, results in hypofertility and seminoma. *Cancer Res.* 2016;76(21):6382-6395.
- Li N, Cai Y, Zou M, et al. CFIm-mediated alternative polyadenylation safeguards the development of mammalian pre-implantation embryos. *Stem Cell Reports.* 2023;18(1):81-96.

5. Ran Y, Huang S, Shi J, et al. CFIm25 regulates human stem cell function independently of its role in mRNA alternative polyadenylation. *RNA Biol.* 2022;19(1):686-702.
6. Masamha CP, Xia Z, Yang J, et al. CFIm25 links alternative polyadenylation to glioblastoma tumour suppression. *Nature.* 2014;510(7505):412-416.
7. Xiong M, Chen L, Zhou L, et al. NUDT21 inhibits bladder cancer progression through ANXA2 and LIMK2 by alternative polyadenylation. *Theranostics.* 2019;9(24):7156-7167.
8. Xing Y, Chen L, Gu H, et al. Downregulation of NUDT21 contributes to cervical cancer progression through alternative polyadenylation. *Oncogene.* 2021;40(11):2051-2064.
9. Mills TW, Wu M, Alonso J, et al. Unraveling the role of MiR-181 in skin fibrosis pathogenesis by targeting NUDT21. *FASEB J.* 2024;38(17):e70022.
10. Weng T, Huang J, Wagner EJ, et al. Downregulation of CFIm25 amplifies dermal fibrosis through alternative polyadenylation. *J Exp Med.* 2019;217(2):e20181384.
11. Weng T, Ko J, Masamha CP, et al. Cleavage factor 25 deregulation contributes to pulmonary fibrosis through alternative polyadenylation. *J Clin Invest.* 2019;129(5):1984-1999.
12. Alcott CE, Yalamanchili HK, Ji P, et al. Partial loss of CFIm25 causes learning deficits and aberrant neuronal alternative polyadenylation. *elife.* 2020;9:e50895.
13. Gennarino VA, Alcott CE, Chen CA, et al. NUDT21-spanning CNVs lead to neuropsychiatric disease and altered MeCP2 abundance via alternative polyadenylation. *elife.* 2015;4:e10782.
14. Masamha CP. The emerging roles of CFIm25 (NUDT21/CPSF5) in human biology and disease. *Wiley Interdiscip Rev RNA.* 2023;14(3):e1757.
15. Danckwardt S, Hentze MW, Kulozik AE. 3' end mRNA processing: molecular mechanisms and implications for health and disease. *EMBO J.* 2008;27(3):482-498.
16. Mandel CR, Bai Y, Tong L. Protein factors in pre-mRNA 3'-end processing. *Cell Mol Life Sci.* 2008;65(7-8):1099-1122.
17. Clerici M, Faini M, Muckenfuss LM, Aebersold R, Jinek M. Structural basis of AAUAAA polyadenylation signal recognition by the human CPSF complex. *Nat Struct Mol Biol.* 2018;25(2):135-138.
18. Shi Y, di Giammartino DC, Taylor D, et al. Molecular architecture of the human pre-mRNA 3' processing complex. *Mol Cell.* 2009;33(3):365-376.
19. Sun Y, Zhang Y, Hamilton K, et al. Molecular basis for the recognition of the human AAUAAA polyadenylation signal. *Proc Natl Acad Sci U S A.* 2018;115(7):E1419-E1428.
20. Rügsegger U, Beyer K, Keller W. Purification and characterization of human cleavage factor Im involved in the 3' end processing of messenger RNA precursors. *J Biol Chem.* 1996;271(11):6107-6113.
21. Rügsegger U, Blank D, Keller W. Human pre-mRNA cleavage factor Im is related to spliceosomal SR proteins and can be reconstituted in vitro from recombinant subunits. *Mol Cell.* 1998;1(2):243-253.
22. Zhu Y, Wang X, Forouzmand E, et al. Molecular mechanisms for CFIm-mediated regulation of mRNA alternative polyadenylation. *Mol Cell.* 2018;69(1):62-74.e4.
23. Yang Q, Coseno M, Gilmartin GM, Doublé S. Crystal structure of a human cleavage factor CFIm25/CFIm68/RNA complex provides an insight into poly(A) site recognition and RNA looping. *Structure.* 2011;19(3):368-377.
24. Yang Q, Gilmartin GM, Doublé S. Structural basis of UGUA recognition by the Nudix protein CFI(m)25 and implications for a regulatory role in mRNA 3' processing. *Proc Natl Acad Sci U S A.* 2010;107(22):10062-10067.
25. Masamha CP, Xia Z, Peart N, et al. CFIm25 regulates glutaminase alternative terminal exon definition to modulate miR-23 function. *RNA.* 2016;22(6):830-838.
26. Gruber AR, Martin G, Keller W, Zavolan M. Cleavage factor Im is a key regulator of 3' UTR length. *RNA Biol.* 2012;9(12):1405-1412.
27. Martin G, Gruber AR, Keller W, Zavolan M. Genome-wide analysis of pre-mRNA 3' end processing reveals a decisive role of human cleavage factor I in the regulation of 3' UTR length. *Cell Rep.* 2012;1(6):753-763.
28. Redis RS, Vela LE, Lu W, et al. Allele-specific reprogramming of cancer metabolism by the long non-coding RNA CCAT2. *Mol Cell.* 2016;61(4):520-534.
29. Li X, Ding J, Wang X, Cheng Z, Zhu Q. NUDT21 regulates circRNA cyclization and ceRNA crosstalk in hepatocellular carcinoma. *Oncogene.* 2020;39(4):891-904.
30. Ghosh S, Ataman M, Bak M, et al. CFIm-mediated alternative polyadenylation remodels cellular signaling and miRNA biogenesis. *Nucleic Acids Res.* 2022;50(6):3096-3114.
31. Derti A, Garrett-Engele P, MacIsaac KD, et al. A quantitative atlas of polyadenylation in five mammals. *Genome Res.* 2012;22(6):1173-1183.
32. Cui Y, Wang L, Ding Q, et al. Elevated pre-mRNA 3' end processing activity in cancer cells renders vulnerability to inhibition of cleavage and polyadenylation. *Nat Commun.* 2023;14(1):4480.
33. Neilson JR, Sandberg R. Heterogeneity in mammalian RNA 3' end formation. *Exp Cell Res.* 2010;316(8):1357-1364.
34. Beaudoin E, Freier S, Wyatt JR, Claverie JM, Gautheret D. Patterns of variant polyadenylation signal usage in human genes. *Genome Res.* 2000;10(7):1001-1010.
35. Mayr C. Regulation by 3'-untranslated regions. *Annu Rev Genet.* 2017;51(1):171-194.
36. Friedman RC, Farh KKH, Burge CB, Bartel DP. Most mammalian mRNAs are conserved targets of microRNAs. *Genome Res.* 2009;19(1):92-105.
37. Chekulaeva M, Hentze MW, Ephrussi A. Bruno acts as a dual repressor of oskar translation, promoting mRNA oligomerization and formation of silencing particles. *Cell.* 2006;124(3):521-533.
38. Berkovits BD, Mayr C. Alternative 3[prime] UTRs act as scaffolds to regulate membrane protein localization. *Nature.* 2015;522(7556):363-367.
39. An JJ, Gharami K, Liao GY, et al. Distinct role of long 3' UTR BDNF mRNA in spine morphology and synaptic plasticity in hippocampal neurons. *Cell.* 2008;134(1):175-187.
40. Gruber AR, Martin G, Müller P, et al. Global 3' UTR shortening has a limited effect on protein abundance in proliferating T cells. *Nat Commun.* 2014;5:5465.
41. Martin G, Gruber AR, Keller W, Zavolan M. Genome-wide analysis of pre-mRNA 3' end processing reveals a decisive role of human cleavage factor I in the regulation of 3' UTR length. *Cell Rep.* 2012;1(6):753-763.
42. Fernandez V, Hartmann E, Ott G, Campo E, Rosenwald A. Pathogenesis of mantle-cell lymphoma: all oncogenic roads lead to dysregulation of cell cycle and DNA damage response pathways. *J Clin Oncol.* 2005;23(26):6364-6369.

43. Witzig TE. Current treatment approaches for mantle-cell lymphoma. *J Clin Oncol.* 2005;23(26):6409-6414.
44. Campo E, Jaffe ES, Cook JR, et al. The international consensus classification of mature lymphoid neoplasms: a report from the clinical advisory committee. *Blood.* 2022;140(11):1229-1253.
45. Ogura M. Current treatment strategy and new agents in mantle cell lymphoma. *Int J Hematol.* 2010;92(1):25-32.
46. Navarro A, Royo C, Hernández L, Jares P, Campo E. Molecular pathogenesis of mantle cell lymphoma: new perspectives and challenges with clinical implications. *Semin Hematol.* 2011;48(3):155-165.
47. Cheah CY, Seymour JF, Wang ML. Mantle cell lymphoma. *J Clin Oncol.* 2016;34(11):1256-1269.
48. Kluin-Nelemans HC, Hoster E, Hermine O, et al. Treatment of older patients with mantle cell lymphoma (MCL): long-term follow-up of the randomized European MCL elderly trial. *J Clin Oncol.* 2020;38(3):248-256.
49. Wang M, Munoz J, Goy A, et al. Three-year follow-up of KTE-X19 in patients with relapsed/refractory mantle cell lymphoma, including high-risk subgroups, in the ZUMA-2 study. *J Clin Oncol.* 2023;41(3):555-567.
50. Martin P, Maddocks K, Leonard JP, et al. Postibrutinib outcomes in patients with mantle cell lymphoma. *Blood.* 2016;127(12):1559-1563.
51. Kumar A, Eyre TA, Lewis KL, Thompson MC, Cheah CY. New directions for mantle cell lymphoma in 2022. *Am Soc Clin Oncol Educ Book.* 2022;42:1-15.
52. Wiestner A, Tehrani M, Chiorazzi M, et al. Point mutations and genomic deletions in CCND1 create stable truncated cyclin D1 mRNAs that are associated with increased proliferation rate and shorter survival. *Blood.* 2007;109(11):4599-4606.
53. Masamha CP, Albrecht TR, Wagner EJ. Discovery and characterization of a novel CCND1/MRCK gene fusion in mantle cell lymphoma. *J Hematol Oncol.* 2016;9:30.
54. Kenter AL, Wuerffel R, Kumar S, Grigera F. Genomic architecture may influence recurrent chromosomal translocation frequency in the Igh locus. *Front Immunol.* 2013;4:500.
55. Pileri SA, Falini B. Mantle cell lymphoma. *Haematologica.* 2009;94:1488-1492.
56. Pérez-Galán P, Dreyling M, Wiestner A. Mantle cell lymphoma: biology, pathogenesis, and the molecular basis of treatment in the genomic era. *Blood.* 2011;117:26-38.
57. Masamha CP, Todd Z. Adapting 3' rapid amplification of cDNA ends to map transcripts in cancer. *J Vis Exp.* 2018;133:57318. doi:10.3791/57318
58. Ratnadiwakara M, Änkö ML. mRNA stability assay using transcription inhibition by actinomycin D in mouse pluripotent stem cells. *Bio Protoc.* 2018;8(21):e3072.
59. Marjamaa A, Gibbs B, Kotrba C, Masamha CP. The role and impact of alternative polyadenylation and miRNA regulation on the expression of the multidrug resistance-associated protein 1 (MRP-1/ABCC1) in epithelial ovarian cancer. *Sci Rep.* 2023;13(1):17476.
60. Lugowski A, Nicholson B, Rissland OS. Determining mRNA half-lives on a transcriptome-wide scale. *Methods.* 2018;137:90-98.
61. Kubo T, Wada T, Yamaguchi Y, Shimizu A, Handa H. Knockdown of 25 kDa subunit of cleavage factor Im in HeLa cells alters alternative polyadenylation within 3'-UTRs. *Nucleic Acids Res.* 2006;34(21):6264-6271.
62. Amin HM, McDonnell TJ, Medeiros LJ, et al. Characterization of 4 mantle cell lymphoma cell lines: establishment of an in vitro study model. *Arch Pathol Lab Med.* 2003;127(4):424-431.
63. Zhang S, Jiang VC, Han G, et al. Longitudinal single-cell profiling reveals molecular heterogeneity and tumor-immune evolution in refractory mantle cell lymphoma. *Nat Commun.* 2021;12(1):2877.
64. Yuan S, Zuo W, Liu T, Fu H. The therapeutic synergy of selinexor and venetoclax in mantle cell lymphoma through induction of DNA damage and perturbation of the DNA damage response. *Technol Cancer Res Treat.* 2023;22:15330338231208608.
65. Body S, Esteve-Arenys A, Miloudi H, et al. Cytoplasmic cyclin D1 controls the migration and invasiveness of mantle lymphoma cells. *Sci Rep.* 2017;7(1):13946.
66. Mayr C, Bartel DP. Widespread shortening of 3' UTRs by alternative cleavage and polyadenylation activates oncogenes in cancer cells. *Cell.* 2009;138(4):673-684.
67. Dweep H, Sticht C, Pandey P, Gretz N. miRWalk—database: prediction of possible miRNA binding sites by “walking” the genes of three genomes. *J Biomed Inform.* 2011;44(5):839-847.
68. Sticht C, de la Torre C, Parveen A, Gretz N. miRWalk: an online resource for prediction of microRNA binding sites. *PLoS One.* 2018;13(10):e0206239.
69. Li J-H, Liu S, Zhou H, Qu LH, Yang JH. starBase v2.0: decoding miRNA-ceRNA, miRNA-ncRNA and protein-RNA interaction networks from large-scale CLIP-Seq data. *Nucleic Acids Res.* 2013;42(D1):D92-D97.
70. Yang J-H, Li JH, Shao P, Zhou H, Chen YQ, Qu LH. starBase: a database for exploring microRNA-mRNA interaction maps from Argonaute CLIP-Seq and Degradome-Seq data. *Nucleic Acids Res.* 2010;39(suppl\_1):D202-D209.
71. Zhao N, Qi J, Zeng Z, et al. Transfecting the hard-to-transfect lymphoma/leukemia cells using a simple cationic polymer nanocomplex. *J Control Release.* 2012;159(1):104-110.
72. Hansen SV, Blum MK, Abildgaard N, Nyvold CG. Efficient, non-viral and reproducible protocol for stable knockdown of genes in mantle cell lymphoma cell lines. *Blood.* 2020;136:1-2.
73. Sharova LV, Sharov AA, Nedorezov T, Piao Y, Shaik N, Ko MSH. Database for mRNA half-life of 19 977 genes obtained by DNA microarray analysis of pluripotent and differentiating mouse embryonic stem cells. *DNA Res.* 2009;16(1):45-58.
74. Ogorodnikov A, Levin M, Tattikota S, et al. Transcriptome 3' end organization by PCF11 links alternative polyadenylation to formation and neuronal differentiation of neuroblastoma. *Nat Commun.* 2018;9(1):5331.
75. Lackford B, Yao C, Charles GM, et al. Fip1 regulates mRNA alternative polyadenylation to promote stem cell self-renewal. *EMBO J.* 2014;33(8):878-889.
76. Yao C, Biesinger J, Wan J, et al. Transcriptome-wide analyses of CstF64-RNA interactions in global regulation of mRNA alternative polyadenylation. *Proc Natl Acad Sci U S A.* 2012;109(46):18773-18778.
77. Sun M, Ding J, Li D, Yang G, Cheng Z, Zhu Q. NUDT21 regulates 3'-UTR length and microRNA-mediated gene silencing in hepatocellular carcinoma. *Cancer Lett.* 2017;410:158-168.
78. Mitschka S, Mayr C. Context-specific regulation and function of mRNA alternative polyadenylation. *Nat Rev Mol Cell Biol.* 2022;23(12):779-796.
79. Gruber AJ, Schmidt R, Gruber AR, et al. A comprehensive analysis of 3' end sequencing data sets reveals novel

- polyadenylation signals and the repressive role of heterogeneous ribonucleoprotein C on cleavage and polyadenylation. *Genome Res.* 2016;26(8):1145-1159.
80. Kwon B, Fansler MM, Patel ND, Lee J, Ma W, Mayr C. Enhancers regulate 3' end processing activity to control expression of alternative 3' UTR isoforms. *Nat Commun.* 2022;13(1):2709.
81. Park HJ, Ji P, Kim S, et al. 3' UTR shortening represses tumor-suppressor genes in trans by disrupting ceRNA crosstalk. *Nat Genet.* 2018;50(6):783-789.
82. Tamaddon M, Shokri G, Hosseini Rad SMA, Rad I, Emami Razavi A, Kouhkan F. Involved microRNAs in alternative polyadenylation intervene in breast cancer via regulation of cleavage factor "CFIm25". *Sci Rep.* 2020;10(1):11608.
83. Tan S, Li H, Zhang W, et al. NUDT21 negatively regulates PSMB2 and CXXC5 by alternative polyadenylation and contributes to hepatocellular carcinoma suppression. *Oncogene.* 2018;37(35):4887-4900.
84. Zhou Y, Yang J, Huang L, et al. Nudt21-mediated alternative polyadenylation of MZT1 3'UTR contributes to pancreatic cancer progression. *iScience.* 2024;27(2):108822.
85. Xiao S, Gu H, Deng L, et al. Relationship between NUDT21 mediated alternative polyadenylation process and tumor. *Front Oncol.* 2023;13:1052012.
86. Huang X-D, Chen YW, Tian L, et al. NUDT21 interacts with NDUF52 to activate the PI3K/AKT pathway and promotes pancreatic cancer pathogenesis. *J Cancer Res Clin Oncol.* 2024;150(1):8.

### SUPPORTING INFORMATION

Additional supporting information can be found online in the Supporting Information section at the end of this article.

**How to cite this article:** Khan N, Gupta M, Masamha CP. Characterization and molecular targeting of CFIm25 (*NUDT21/CPSF5*) mRNA using miRNAs. *The FASEB Journal.* 2025;39:e70324. doi:[10.1096/fj.202402184R](https://doi.org/10.1096/fj.202402184R)